CULEX: a Cable-driven Upper Limb Exoskeleton for rehabilitation

André F.S. de Araujo
Faculdade de Engenharia Elétrica
Universidade Federal de Uberlândia
Uberlândia, Brazil
ORCID: 0000-0002-5297-9500

Luiz R.R. Carneiro
Faculdade de Engenharia Mecânica
Universidade Federal de Uberlândia
Uberlândia, Brazil
ORCID: 0000-0003-1218-1585

Davi da S. Estrela
Faculdade de Engenharia Mecânica
Universidade Federal de Uberlândia
Uberlândia, Brazil
ORCID: 0000-0001-6800-1219

Alcimar B. Soares
Faculdade de Engenharia Elétrica
Universidade Federal de Uberlândia
Uberlândia, Brazil
ORCID: 0000-0003-1100-3533

Sérgio R. de J. Oliveira
Faculdade de Engenharia Elétrica
Universidade Federal de Uberlândia
Uberlândia, Brazil
ORCID: 0000-0003-2294-2018

***Abstract*— In this paper was proposed a Cable-driven Upper Limb Exoskeleton (CULEX) with 8 degrees of freedom for rehabilitation of patients post stroke with a motor or sensitive dysfunction. With the tension Amplification Mechanism, it was able to transmit the power to the joint and move the motor to a position closer to the shoulder, moving the center of mass with them, making a safer human-robot interaction. Furthermore, it was shown the study of upper limb biomechanics applied to assistive devices, involving the study of range of motion, length and center of mass of the limbs. A 3D printed prototype was made for the validation of the tension-amplification mechanism, and the latest CAD (Computer Aid Design) version had an increase in the moment of inertia of the structure and the separation of the cable system into different section planes for each joint movement.**

Keywords — Exoskeleton, Cable System, Upper Limb, Stroke, Rehabilitation.

I. INTRODUCTION

The stroke is the second cause of death in the world among adults and occurs when a partial or total interruption of blood flow to the brain. Unfortunately, 75% of these subjects develop a motor and or sensitive incapacity. The physiotherapy can mitigate the sequelae of stroke mainly during the first three months due to the neuroplasticity, with emphasis in the first month of rehab [1,2]. However, the traditional manually assisted therapy needs a qualified health professional, being expensive [3] and has a short time session duration.

In order to aid the people who suffer from stroke to restore the Activities of Daily Living (ADL) the exoskeletons were developed. Thus, there are many upper limb exoskeleton [3-11] for people who suffered from stroke or a spinal cord injury. The exoskeleton technology can be used for several applications, such as: a therapeutic and diagnostics device for physiotherapy, an assistive (orthotic) device for human power amplifications, a haptic device in virtual reality simulation, and a master device for teleoperation [4].

In the literature there are many types of exoskeleton mechanisms using electric motors in the joint or using cable systems or even pneumatics actuators to make all the Degrees of Freedom (DoF) movements. By reason of the high weight of the motors and high inertial due to its position in the joint, besides the low stiffness of the cable. Kim developed a cable-driven system for a robot arm (LIMS) with reduction in the joints which solve these troubles [12].

According to Xiao et al, some cable-powered exoskeletons found in literature have a large structure that supports the cable actuators [3], limiting the applications environment. The structure proposed in CAREX [7] and MEDARM [10] needs a huge static structure to support the motors and actuators, as the force transmission mechanism. Besides that, CABXLexo-7 [3], CADEN [4] and Armin II [11] present a cable system which uses a structure to support all the motors that makes the wearability more difficult.

To assist the control of these machines, commonly used human-robot interfaces (HRI) and smart algorithms capable of identifying the user's movement intentions [11]. For exoskeleton control it is typically used Electro - Encephalography (EEG) [14], Electromyography (EMG) [15,16], force/torque sensor [16] and Force-Sensing Resistor (FSR) [17] to aid extract the movement intentions.

Therefore, the objective of this work is to develop a lightweight and comfortable exoskeleton (CULEX) with 8 DoF operated by cables, for motor rehabilitation of post-stroke patients. Introducing an optimized mechanical system capable of performing compound movements based on the study of human biomechanics for safe interaction with motor difficulties patients.

II. MATERIALS AND METHODS

A. *Biomechanical of Upper Limb*

To start this work it was necessary to establish the DoF of the upper limb. The upper limb can be represented with a total of 9 DoF without the finger joints, of which there are 5 DoF for shoulder, 2 for elbow and 2 for wrist [18].

In this representation, the shoulder has the sternoclavicular joint with 2 DoF, this joint has Shoulder Retraction (SRE) / Protraction (SPR) {J1} and Elevation (SEL) / Depression (SDE) {J2}. In the shoulder there is also the glenohumeral joint which is responsible for 3 DoF, Shoulder Abduction (SAB) / Adduction (SAD) {J3}, Flexion (SF) / Extension (SE) {J4} and Internal (SIR) / External Rotation (SER) {J5}. The elbow complex has 2 DoF, Elbow Flexion (EF) / Extension (EE) {J6} and Forearm Pronation (FP) / Supination (FS) {J7}. Lastly the wrist joint has 2 DoF, Wrist Flexion (WF) / Extension (WE) {J8} and Radial (WRD) / Ulnar Deviation (WUD) {J9} [18,19]. All this DoF can be visualized in Fig. 1.

With the aim of simplifying the complexity of the system, the exoskeleton of this project will have 8 DoF instead of 9 DoF, and will suppress the shoulder elevation / depression {J2}. Normally the design of exoskeletons suppress sternoclavicular DoF, due to the short range of these movements, a simple good solution is to use a passive joint

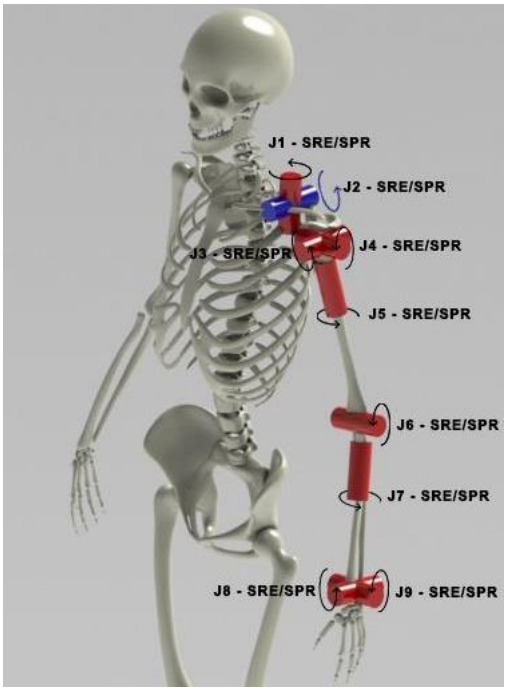

Fig. 1. Illustration of 9 Degrees of Freedom of the upper limb. Author.

which can promote a free movement for this joint [5]. However, in future works are intended to use CULEX as a robot arm, so all joints must be controlled by a motor.

To build the exoskeleton it was necessary to know the angles of the Range of Motion (RoM) of each DoF. These values can be found in the literature with slight variation [3,4,6,19], like in the shoulder flexion (SF) RoM is between 130º-180º and the shoulder extension (SE) RoM is between 30º-80º. In order to obtain the most general conditions, it was considered the biggest RoM for each DoF to build the RoM Human column of Table 1.

To determine the torque in each joint, it was necessary to know the length, the Center of Mass (CoM) and the weight of the arm, forearm and hand. Thus, it was considered the weight and height of a man with 2 m and BMI (Body Mass Index) of 25, which is the beginning of overweight with approximately 100 kg. These conditions were stipulated in order to cover a large portion of users who are below these conditions, generating a safety margin for various applications with CULEX. In the literature we found the estimated location of the CoM for the hand, forearm and arm [20]. Therefore, in table 2 below, it presents the Length, CoM from the center of rotation of the shoulder for each part, as well as its weight.

B. *Used Material*

For the main structure of the exoskeleton the stiffness and strength of material must be high due to the high mechanical demand in it, since the inertia in the structure is high. Seeking a rapid prototyping of relatively complex structures, the 3D printing method has become the best option at this stage of the research, having a range of materials that cover different needs. Thus, ABS was chosen to print the prototype due to its good mechanical strength, tenacity, low density and relatively cheap, however the warping in ABS is higher than in other materials due to its shrinkage rate.

In order to transfer the power from the motor to the joint, some types of cables were considered, analyzing their resistance limit vs. weight. These properties were analyzed firstly for the steel cable, which has high tensile strength and high specific weight. On the other hand, the properties of the multifilament PE (polyethylene) fishing line were analyzed, which has high tensile strength due to its application, is lighter than steel, and has no memory effect. Thus, due to its properties and malleability, the multifilament fishing line presented is more suitable for this application.

TABLE 1. RANGE OF MOTION OF THE HUMAN UPPER LIMB AND OUR EXOSKELETON.

Degrees of Freedom	Joints	RoM Human (degrees)	RoM Exoskeleton (degrees)
SRE /SPR	J1	-	5/15
SAB /SAD	J3	180/50	120/30
SF / SE	J4	130-180/30-80	150/60
SIR / SER	J5	70-95/40-70	70/90
EF / EE	J6	140-146/0	180/0
FP / FS	J7	85-90/70-90	-
WF / WE	J8	90/80	-
WRD / WUD	J9	15/30-40	-

TABLE 2. CENTER OF MASS AND WEIGHT OF THE UPPER LIMBS PARTS.

Parts	Length (m)	Shoulder distance to CoM (m)	Mass (Kg)	Weight (N)
Arm	0,372	0,162	3,25	31,88
Forearm	0,292	0,498	1,87	18,34
Hand	0,216	0,771	0,65	6,38

The cable powered system exoskeletons founded in the literature generally use pulleys to reduce friction, route the cables [3,4,7] and increase power by associating pulleys to create a tension-Amplification Mechanism [12]. To minimize friction between the pulley and the shaft, pulleys with bearings can be used, maximizing the efficiency of the cable system.

C. *Safety Requirements*

As it is a mobile system, the exoskeleton needs movement limiters to ensure the wearer's safety. Thus, preventing accidents by exceeding the limits of the degrees of freedom of human joints. Three restrictive measures were proposed for this: first, a mechanical restriction, such as physical contact; second, a limitation by means of software, calculating the angle and allowing movement within a specific range; and third, an electrical limitation, which will cut the power supply if the other two measures are not sufficient. With these measures, the user will be able to use the exoskeleton reducing complications and eventual accidents.

All RoM of the exoskeleton will be bio-inspired on the human RoM anatomy as shown in Table 1 to reduce the

chance of an accident due to hyperextend or hyperflex of the joints [4].

Another important factor to the safety of the user of the exoskeleton is to reduce injury of human-robot interaction. To reduce this injury is necessary to reduce the total transferring energy, and it is possible by minimizing the robot inertia. A simple way to do this is using the cable system to transfer the power of the motor and increase the stiffness of the joints [12].

III. EXOSKELETON DESIGN

Taking into account the positioning of the upper limb DoF the exoskeleton was developed with J1, J3, J4, J5 and J6 joints, mimicking human joints in position and RoM, as shown in Fig. 2.

A. *Cable System*

The joint design was based in tension- Amplification Mechanism as shown in Fig. 3(a). This mechanism allows use of just one motor far from the joint to make the respective agonist and antagonist motion, moving the Center of Mass (CoM) closer to the shoulder and increasing the wearability.

Associating a couple of pulleys in the same joint increases linearly the tension (1) and quadratic the stiffness (2) by the same number of wires turning around pulleys (n). In this way, the tension of the actuator T_{in} will be amplified n-times and resulting in the tension on the joint T_{out}.

$$T_{out} = n \times T_{in} \tag{1}$$

$$K_{out} = \frac{T_{out}}{\Delta x_{out}} = \frac{n \times T_{int}}{\Delta x_{in}/n} = n^2 \times \frac{T_{in}}{\Delta x_{in}} = n^2 \times K \tag{2}$$

The stiffness (K) of the cable is the result of the tension (T_{in})in it by the shortening of the cable (Δx_{in}), and the stiffness (K_{out}) of the joint is the result of the tension (T_{out}) in it by the shortening of the cable between the pulleys (Δx_{out}). We can notice that the reduction in the length of the cable in the motor (Δx_{in}) is n-times larger than the reduction between the pulleys of the joint (Δx_{out}), as shown in Fig. 3(b).

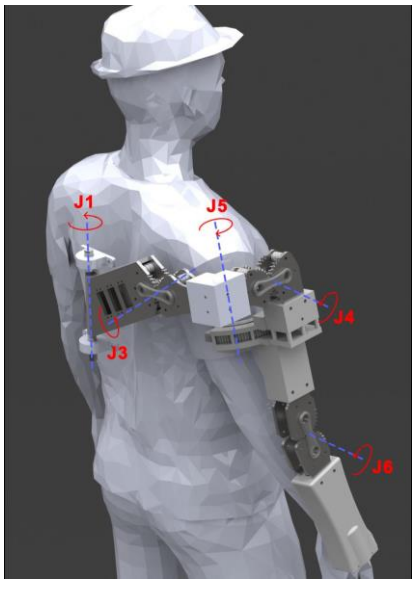

Fig. 2. Illustration of Degrees of Freedom of CULEX. Author.

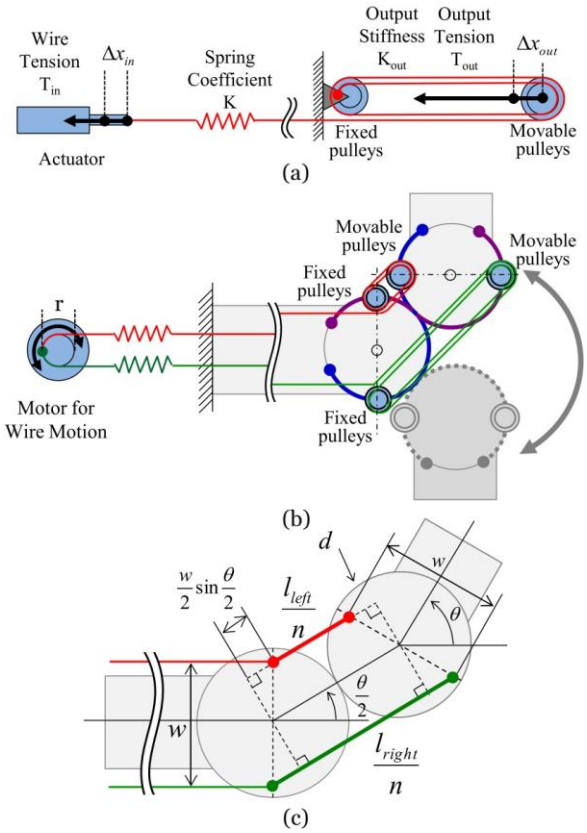

Fig. 3. (a) Tension-Amplification Mechanism for 1 DoF on the joint. (b) Basic Tension-Amplification Mechanism. (c) Mechanical schematic for 1 DoF joint [10]

Furthermore, these mechanisms increase the torque in the joint by the relation of tension amplification (n), radius of the motor shaft (r_{motor}), distance between the pulleys (w) and the relative angle (θ) (3). The visualization of these variables is presented in Fig. 5.

$$\frac{t_{joint}}{t_{motor}} = \frac{n \times w}{2 \times r_{motor}} \times \cos\left(\frac{\theta}{2}\right) \tag{3}$$

For this project it used r_{motor}= 3,5 mm, n=3, w=55 mm, and θ=[-100º,110º]. It results in a maximum and minimum torque amplification of 23,5 folds and 13,52 folds respectively. This torque changes by the movement of the joint which changes the θ angle, as shown in Fig. 4.

The torque of a limb relative to a joint is calculated from the distance between the centroid of that limb to the desired joint multiplied by the weight of this limb. Thus, to calculate the total torque in a given joint, it is possible by making the sum of the torque generated by all posterior members to the desired joint. Thus, to calculate the torque on the wrist, only the torque of the hand in relation to the wrist should be taken into account. In the case of the elbow, the torque of the hand and forearm in relation to the elbow must be considered, and for the shoulder, the torque of the hand, forearm and arm in relation to the shoulder must be considered.

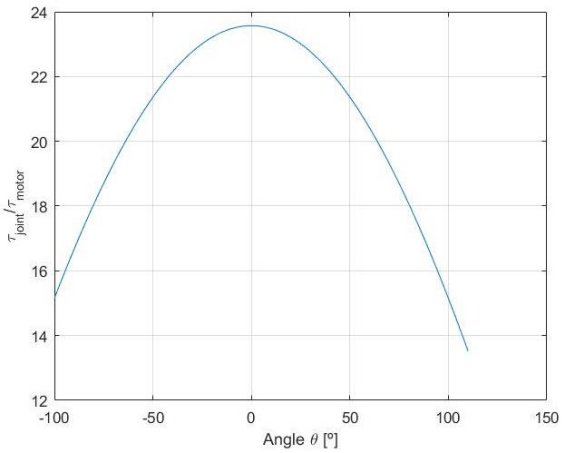

Fig. 4. Torque amplification due to angular variation (θ).

By using the torque amplification and the necessary torque and angular velocity for each joint (Table 3), were possible to choose the motor which will be used in the final version of the exoskeleton. It was decided to use a brushless motor mainly due to the higher torque to weight ratio compared with brushed motors.

Inspired by LIMS [12], this strategy can be used to move the motors near to the shoulder and allow the shoulder abduction / adduction, flexion / extension and elbow flexion / extension in CULEX joints as shown in Fig. 2 J3, J4 and J6 respectively.

The mechanism implemented in J3 can be visualized in the Fig. 5, this is one of the most complicated joint due to the highest number of cable which pass through the middle of the joint to control J4 (red) and J5 (blue), besides there are the cable which will promote their own motion (green). The red and blue cables will cross the joint through two pulleys, which will maintain the length and the tension of these cables independently of the motion of the joint, but to guarantee this condition, the cable must remain tangent with the pulleys along its path. To maintain this tangence it used two extra pulleys that are closer to the motor. It is important to inform that these motors in Fig. 5 represent the position of the motor shaft and in its place will be used brushless motor.

To avoid contact between the cables, each joint movement was separated into different geometric planes with its respective cable system, allowing the performance of compound movements. In Fig. 6 it can be visualized that the J4 movement is made by the red cable which is in a different section plane than the blue cable that passes forward to the J5 joint.

B. Structure

TABLE 3. TORQUE, ANGULAR VELOCITY AND POWER OF EACH JOINT.

Joint	Torque (N.m)	Angular velocity (rad/s)	Power (W)
Shoulder	32,7	1,05	34,21
Elbow	8,3	1,05	8,64
Wrist	1,2	2,09	2,43

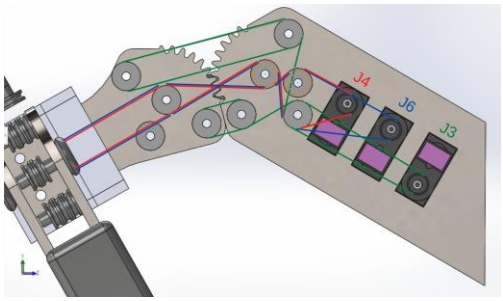

Fig. 5. Mechanical system and cable passage, green for J3, red for J4 and blue for J6.

The mechanism proposed in Fig. 3 needs a cable or a gear contact to avoid slipping between the surfaces. For this project it was chosen as a gear solution due to the manufacturing method used in the prototype (3D printing) and the future method for the final version (machining). Both methods permit manufacturing the teeth of the gears, which will reduce the slipping in comparison with the cable which has some elasticity.

A reduction in the inertia of the system can be made positioning all the motors as close to the shoulders as possible, moving up the CoM with them. This strategy can reduce the rotation inertia in addition to reducing the torque in the joints allowing the use of light motors as done in LIMS [21]. As said in safety requirements, the reduction in the inertia of the system allows a safer human-robot interaction.

Furthermore, it is important to inform that J3, J4 and J6 have not only rotation but also a small translation. It is caused by the effect of one gear translating around the other. It is not a problem for J3 and J4 joints because these transactions can be interpreted as the rotation of J2 which aren't implemented in CULEX.

The first iteration of CULEX was 3D printed with a 20% reduction in size to validate the cable-driven system, the energy lost due to the friction in the pulleys, the structural inertia and integrity. This printed version can be seen in Fig. 7.

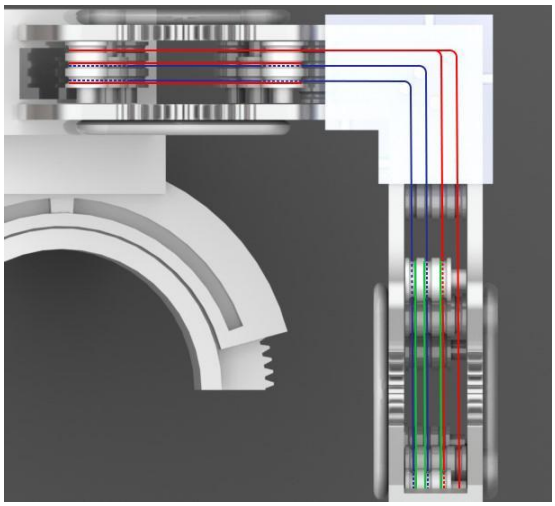

Fig. 6. Upper view of the exoskeleton to visualize the different section planes of pulleys.

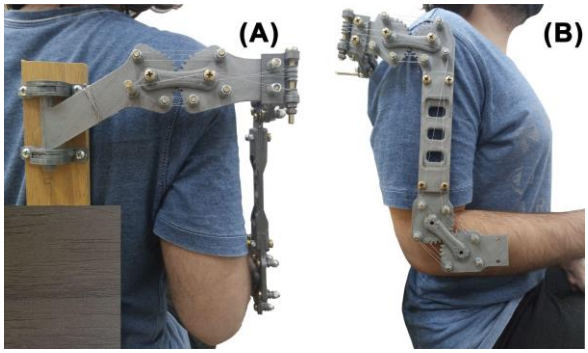

Fig. 7. (a) Lateral view of the 3D printed prototype. (b) Rear view of the 3D printed prototype.

To improve the reliability of the structure, increasing its rigidity is essential. The stiffness is the resistance to deflection or deformation of an elastic body by an applied force. There are many ways to change the stiffness of a structure, by changing the base material or changes in geometry and its cross-sectional area by varying its moment of area.

After the first iteration of CULEX, an increase in the moment of area of the structure was proposed by incorporating a double plate joint extending the distance between the CoM of these cross sections, as it is possible to increase its moment of inertia by the quadratic distance of the CoM in the perpendicular direction by the parallel axis theorem [22].

The Fig. 2, 5 and 6 are the latest versions of the project with many improvements due to the troubles found during the validation of the first version of the prototype (Fig. 7).

IV. Discussion

This article contributes to the development of the field by the design of a low inertia cable-driven exoskeleton reducing the injury of human-robot interaction. Furthermore, it was shown the study of upper limb biomechanics applied to assistive devices, involving the study of RoM, length and CoM of the limbs.

As shown in Table 1, the RoM of J1, J3, J4, J5 and J6 of CULEX are mimicking the human joint position and RoM found in the literature. The J3 joint has a RoM slightly shorter than the human RoM due to the mechanical limitation of that joint. Besides that, the mechanism used for the SIR/SER {J5} is composed of some gears, since the movement of this DoF takes place with an axis parallel to the passage of the cables. Yet, J3, J4 and J6 joints have a translation which can be mitigated by reducing the primitive diameter of the joint gear.

It was observed in the first printed model a slack in the cable system, to overcome the challenges, a pre-tension mechanism will be implemented [3] in order to prevent the reduction in the stiffness of the structure. Moreover, a standard cable-driven system presents a considerable malleability, however the tension amplification mechanism can increase the stiffness of the joint reducing this problem [12].

Thus, CULEX is an exoskeleton with 8 DoF which can be used in many applications, mainly to mitigate the sequelae of stroke in addition to the workout of the separate muscular groups. The exoskeleton can provide the movements of several DoF simultaneously, as seen in Fig. 2, and together with current physiotherapy methods, they seek to improve the neuroplasticity of stroke patients by restoring more complex movements than those currently achieved in conventional physiotherapy.

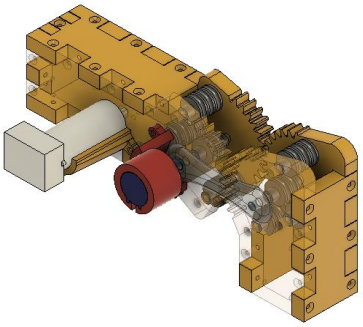

Fig. 8. Control prototype joint.

V. Future Works

The next step of this project will be to print a mini setup of a joint (Fig. 8) to test a control loop algorithm for the cable-driven system presented in this paper, the proposed control loop block diagram is shown in Fig. 9. The Proportional–integral–derivative (PID) was chosen due to the simple steps to achieve a good result without modeling all variables of the system. Furthermore, it is intended to use the Fuzzy logic to aid the controller to reduce error due to the variance in the plant dynamic by reason of the many different users that will use the CULEX.

Moreover, a potentiometer will be used due to its simplicity and high resolution compared to an encoder of the same size. This potentiometer will be coupled to the bar that connects the two gears of the joint and will measure the half variation of the angle ($\theta/2$).

To close the control loop, an ESP32 microcontroller will be used because of its two cores, it will facilitate in the future the communication of a network of microcontrollers. Each joint will use an ESP32, and an additional master ESP32 to calculate the reference angle by an inverse kinematic algorithm.

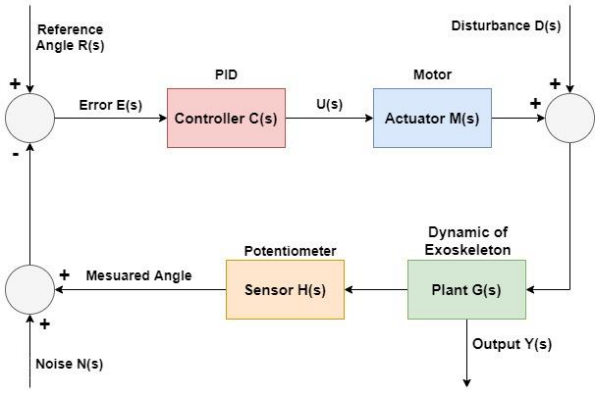

Fig. 9. Control loop block diagram of one joint

After that, the design of the remaining DoF (J7, J8, J9) will be developed, even as the scaling by finite element simulation. Finally, the printing and assembling of CULEX will be made, as well as the final implementation of your control loop.

The final step of this project will be the clinical trial of CULEX for rehabilitation of post-stroke patients, providing an aid for the upper limb motion. Hence, the exoskeleton can be used to increase or decrease the load during the patient's movements in the physiotherapy, stimulating the neuroplasticity of the motor region of the brain.

VI. CONCLUSION

Owing to all the sections presented in this paper, show that CULEX had great improvements in its development. The exoskeleton DoF design meets the positioning and constraints of human upper limb biomechanics.

Moreover, it was shown that the tension amplification mechanism provided a 20 folds increase in the torque applied by the motor to the joint. In the first iteration of the printed prototype was observed the independence of the cable-system for each joint, besides the satisfactory stiffness for these joints. In addition, the displacement of the motors to a region close to the shoulder allowed a reduction in torque on the joints, as well as a reduction in the inertia generated by them as mentioned in safety requirements.

There are several future steps to complete this project, such as finalizing the remaining DoF, implementing the control law as well as the inverse kinematics algorithm, as mentioned in the previous section.

ACKNOWLEDGMENT

The authors wish to acknowledge Y.-J. Kim and J. C. Perry for their vital contributions to the work. Moreover, the study was supported by Laboratório de Engenharia Biomédica da Universidade Federal de Uberlândia.

REFERENCES

1. R. da S. Aramaki, Análise da recuperação funcional no acidente vascular encefálico isquêmico após 30 dias de reabilitação em unidade pública de saúde.Uberlândia, Universidade Federal de Uberlândia, 2019. http://dx.doi.org/10.14393/ufu.di.2019.978.
2. C. R. Gonçalves, Protocolo 3D para avaliação quantitativa de déficits proprioceptivos. Uberlândia, Universidade Federal de Uberlândia, 2018. http://dx.doi.org/10.14393/ufu.di.2018.1226.
3. F. Xiao, Y. Gao, Y. Wang, et al. (2018) Design and evaluation of a 7-DOF cable-driven upper limb exoskeleton. Journal of Mechanical Science and Technology, vol. 32, pp 855–864. https://doi.org/10.1007/s12206-018-0136-y.
4. J. C. Perry, J. Rosen and S. Burns (2007), Upper-Limb Powered Exoskeleton Design. IEEE/ASME Transactions on Mechatronics, vol. 12, no. 4, pp 408-417. https://doi.org/10.1109/TMECH.2007.901934.
5. Ho Shing Lo, Sheng Quan Xie, Exoskeleton robots for upper-limb rehabilitation: State of the art and future prospects. Medical Engineering & Physics, vol. 34, issue 3, pp 261-268, 2012. https://doi.org/10.1016/j.medengphy.2011.10.004.
6. Y. Chen et al. "Design of a 6-DOF Upper Limb Rehabilitation Exoskeleton with Parallel Actuated Joints". Bio-Medical Materials and Engineering, vol. 24, no. 6, pp 2527–2535, September 2014. https://doi.org/10.3233/BME-141067.
7. Y. Mao, S. K. Agrawal, "Design of a cable-driven arm exoskeleton (CAREX) for neural rehabilitation," IEEE Transactions on Robotics, vol 28, pp 922–931, August 2012. https://doi.org/10.1109/TRO.2012.2189496.
8. M. Gunasekara, R. Gopura, S. Jayawardena, (2015) "6-REXOS: Upper limb exoskeleton robot with improved pHRI," International Journal of Advanced Robotic Systems, vol. 12, issue 4, May 2017. https://doi.org/10.5772/60440.
9. Y. Jung, and J. Bae, "Kinematic analysis of a 5-DOF upper-limb exoskeleton with a tilted and vertically translating shoulder joint," IEEE/ASME Transactions on Mechatronics, vol. 20, issue 3, pp 1428–1439, June 2015. https://doi.org/10.1109/TMECH.2014.2346767.
10. S. J. Ball, I. E. Brown, and S. H. Scott, (2007). MEDARM: A rehabilitation robot with 5DOF at the shoulder complex, In IEEE/ASME International Conference on Advanced Intelligent Mechatronics, AIM, Zurich, Switzerland, 2007. https://doi.org/10.1109/AIM.2007.4412446.
11. M. Mihelj, T. Nef, and R. Riener, (2007). ARMin II - 7 DoF rehabilitation robot: Mechanics and kinematics, In Proc. IEEE International Conference on Robotics and Automation, Rome, Italy, 2007, pp. 4120–4125. https://doi.org/10.1109/ROBOT.2007.364112.
12. Y.-J. Kim, "Anthropomorphic Low-Inertia High-Stiffness Manipulator for High-Speed Safe Interaction," IEEE Transactions on Robotics vol. 33, issue 6, pp 1358-1374, December 2017. https://doi.org/10.1109/TRO.2017.2732354.
13. E. Trigili, L. Grazi, S. Crea, et al. "Detection of movement onset using EMG signals for upper-limb exoskeletons in reaching tasks," Journal of NeuroEngineering and Rehabilitation, vol. 16, March 2019. https://doi.org/10.1186/s12984-019-0512-1.
14. N. A. Bhagat, A. Venkatakrishnan, B. Abibullaev, et al. (2016) Design and optimization of an EEG-based brain machine interface (BMI) to an upper-limb exoskeleton for stroke survivors. Frontiers in Neuroscience vol. 10. https://doi.org/10.3389/fnins.2016.00122.
15. A. Krasoulis, S. Vijayakumar, and K. Nazarpour, "Multi-Grip Classification-Based Prosthesis Control with Two EMG-IMU Sensors," IEEE Transactions on Neural Systems and Rehabilitation Engineering vol. 28, issue 2, pp 508–518, February 2020. https://doi.org/10.1109/TNSRE.2019.2959243.
16. K. Kiguchi, and Y. Hayashi, "An EMG-based control for an upper-limb power-assist exoskeleton robot," IEEE Transactions on Systems, Man, and Cybernetics, Part B: Cybernetics vol. 42, issue 4, pp 1064–1071, august 2012. https://doi.org/10.1109/TSMCB.2012.2185843.
17. J. Huang, W. Huo, W. Xu, et al. "Control of Upper-Limb Power-Assist Exoskeleton Using a Human-Robot Interface Based on Motion Intention Recognition," IEEE Transactions on Automation Science and Engineering vol. 12, issue 4, pp 1257–1270, October 2015. https://doi.org/10.1109/TASE.2015.2466634.
18. B. Tondu, "Estimating shoulder-complex mobility," Applied Bionics and Biomechanics vol. 4, no. 1, pp 19–29, 2007. https://doi.org/10.1080/11762320701403922.
19. J. L. Pons, Wearable Robots: Biomechatronic Exoskeletons, 1st ed., SoutherGate, Chichester, John Wiley & Sons Ltd, England, 2008.
20. W. T. Dempster, Space requirements of the seated operator. WADC Technical Report vol. 16, pp.55-159, 1995, Wright-Patterson Air Force Base, Ohio.
21. Y.-J. Kim, (2015) Design of low inertia manipulator with high stiffness and strength using tension amplifying mechanisms, in IEEE International Conference on Intelligent Robots and Systems, 2015, pp. 5850–5856. https://doi.org/10.1109/IROS.2015.7354208
22. F. P. Beer, E. R. Johnston Jr, D. F. Mazurek, et al, Mecânica Vetorial para Engenheiros: Estática, 9ª ed, AMGH Editora Ltda , 2011, pp. 474-53